THE ELECTROMAGNETIC STRUCTURE OF THE NUCLEON

U. Meyer-Berkhout,
Deutsches Elektronen-Synchrotron, Hamburg

During the past ten years electron-nucleon scattering experiments have provided convincing evidence that the nucleon has structure. In other words, the observed scattering of high-energy electrons from nucleons is quite different from the scattering that would be expected if the proton and neutron were point particles with their actual charges and magnetic moments. The term "structure" is somewhat misleading in that it may convey the idea of some kind of measurable spatial distribution of charge and current inside the nucleon. As was discussed in Dr. Beckmann's lectures, it is better to avoid such spatial concepts, since the principles of relativity and quantum mechanics imply that it is difficult to attach a meaning to them. The results of electron scattering experiments are scattering amplitudes as function of the momentum of the incident and scattered electron. These scattering amplitudes can be expressed in terms of the electromagnetic form factors. Limiting ourselves to the electromagnetic electron-nucleon interaction, the electromagnetic structure of the nucleon in its ground state is fully described by a total number of four form factors which are functions only of q^2, the Lorentz-invariant squared energy-momentum transfer. In the early times of electron scattering work, one used the Dirac and Pauli form factors $F_1(q^2)$ and $F_2(q^2)$ for proton and neutron. At present, the electric and magnetic form factors of proton and neutron $G_E(q^2)$ and $G_M(q^2)$ are preferred. These are linear combinations of the Dirac and Pauli form factors

$$G_E(q^2) = F_1(q^2) - \frac{q^2}{4M^2}\kappa F_2(q^2) \qquad G_M(q^2) = F_1(q^2) + \kappa F_2(q^2) .$$

The four form factors - two for the proton and two for the neutron - are sufficient to account for elastic electron-nucleon scattering, and there is absolutely no reason to introduce the concept of spatial structure. However, implicitly one frequently falls back into the habit of using spatial concepts. For example, when we ask whether there exists a central core in the charge or magnetic moment structure of the proton, we are using a spatial concept, but we really mean the behaviour of the proton form factors at large momentum transfers.

In this talk it will be assumed that you are familiar with the definition of the form factors. Furthermore, some knowledge of the Rosenbluth equation gives the differential cross-section for elastic electron-nucleon scattering. The basic underlying assumptions upon which the derivation of the Rosenbluth equation is based are:

1. Pure electromagnetic interaction between the electron (or muon, which is also used as a probe) and the nucleon. In other words, it is assumed that all other electron-nucleon interactions (e.g. weak interaction) can be neglected. The assumption is justified in the presently accessible energy range.

2. Validity of quantum electrodynamics. In principle it is possible that part of the observed structure, that is part of the variation of the form factors with q^2, arises from a break-down of quantum electrodynamics. However, this is not very likely since quantum electrodynamics has been tested thoroughly in experiments involving essentially only muons and electrons. One good but incomplete check is the comparison of the scattering of muons and electrons by protons or heavier nuclei at the same four momentum transfer. This will measure the ratio of the muon to electron electromagnetic form factors because all other parts of the Feynman diagram are the same. Such experiments have been done at CERN and at Brookhaven National Laboratory. The results indicate that in the thus far investigated range of four momentum transfers which extends up to about 1 $(GeV/c)^2$ no measurable differences exist between the electron and muon vertex functions. Although quite a few additional experiments have been carried out to test the validity of quantum electrodynamics, one still does not know whether quantum electrodynamics will eventually break down at very high momentum transfers. From our point of view, such a break-down could result either in a change of the photon propagator $1/q^2$ or a deviation of the electron (or muon) form factor from unity at high momentum transfers. In fact, unexpected results were obtained in a recent experiment performed by Blumenthal et al.[1] at the Cambridge electron accelerator on wide-angle production of symmetrical electron pairs produced by photon in a carbon target. In this experiment, deviations from the predictions based on the Bethe-Heitler equation are observed[1]. If confirmed, it may mean a break-down of quantum electrodynamics. But it is too early to make such a drastic statement since a great many corrections enter into the experiment and the results are still of a preliminary nature. One may also hope to learn more about the validity of quantum electrodynamics from colliding beam electron-electron scattering experiments now being performed with the Stanford storage rings. For the time being we shall be naive and assume that electrons and muons have no structure, whereas the strongly interacting nucleon has structure which is associated with the cloud of strongly interacting particles surrounding the nucleon. Our simple-minded approach implies admitting that we do not have the slightest idea of what is the origin of the mass difference between electron and muon.

3. The third basic assumption upon which the derivation of the Rosenbluth equation is based is the one-photon exchange approximation. It is assumed that the elastic electron-nucleon interaction is mediated by the exchange of a single virtual photon. Two-photon exchange processes which in principle can contribute to the elastic $e-\mathcal{N}$ cross-section are neglected. At first sight it may seem reasonable to assume that contributions due to two-photon exchange graphs are small, since they are reduced by one power of $\alpha = 1/137$ relative to the one-photon exchange contribution. However, we shall see that the situation is not quite that simple. We shall have to come back later to the problem of justifying the one-photon exchange approximation.

In the one-photon exchange diagram the circle around the proton vertex is meant to indicate that no attempt is made to specify in detail how the interaction occurs. The blob simply symbolizes all effects of any number of strongly interacting virtual particles which contribute to nucleon structure.

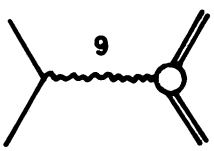

The four momentum of the virtual photon is given by

$$q = \{\vec{q},\ q_0\}\ ,$$

where q is the transferred momentum and $q_0 = i\Delta E$ the transferred energy. Units are used in which h = c = 1. The Lorentz-invariant square of the four-momentum transfer is then given by

$$q^2 = (\vec{q})^2 - \Delta E^2\ .$$

In electron nucleon scattering experiments one is dealing with spacelike four-momentum transfers. If using this metric which was also used by Dr. Beckmann in his lectures one has positive q^2 values for electron-nucleon scattering. For the crossed-reaction - nucleon-antinucleon annihilation to electron-positron pairs - the four momentum of the intermediate photon is timelike, i.e. q^2 is negative and smaller than $-4M^2$. This is immediately obvious in the centre-of-mass system in which the four-momentum transfer has only space components for elastic electron-nucleon scattering since $\Delta E = 0$. In other words, as long as we have elastic scattering the virtual photon carries no energy but only momentum in the centre-of-mass system. In the crossed channel the intermediate photon carries no momentum but only energy in the centre-of-mass system. Since the square of the transferred energy must be at least $4M^2$ one has $q^2 \geq 0$ and $q^2 \leq -4M^2$.

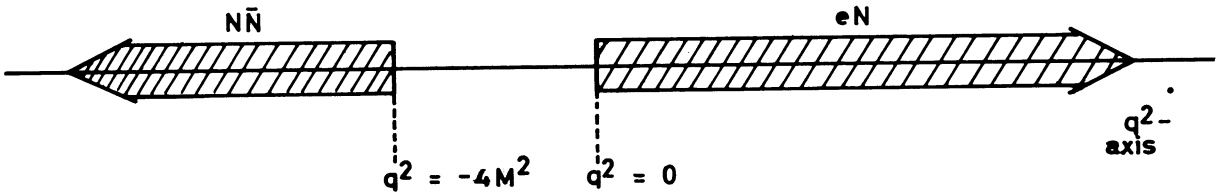

Dr. Zichichi will discuss what is known about the behaviour of form factors in the region of time-like momentum transfers. Therefore, we can limit ourselves here to a discussion of the form factors in the region of space-like four-momentum transfers.

The Rosenbluth equation expresses the differential cross-section $d\sigma/d\Omega$ for elastic scattering through an angle Θ in the laboratory system

$$\frac{d\sigma}{d\Omega} = \left(\frac{d\sigma}{d\Omega}\right)_{NS}\left[\frac{G_E^2 + \tau G_M^2}{1+\tau} + 2\tau G_M^2 \operatorname{tg}^2\frac{\Theta}{2}\right]\ .$$

The Rosenbluth equation contains only two adjustable parameters which are the two form factors $G_E(q^2)$ and $G_M(q^2)$ describing the photon-proton interaction. In case of electron-neutron scattering these form factors have to be replaced by the corresponding neutron form factors. For space-like momentum transfers, information on the behaviour of the four nucleon form factors is available up to momentum transfers of 6.81 $(GeV/c)^2$. When expressed in units of an inverse squared length this corresponds to a q^2 value of 175 f^{-2} [1 $(GeV/c)^2 \hat{=} 25.7\ f^{-2}$]. The symbol τ is used to denote the invariant squared four-momentum transfer q^2 divided by $4M^2$ where M is the mass of the nucleon:

$$\tau = \frac{q^2}{4M^2}\ .$$

If q^2 is expressed in units of $(\text{fermi})^{-2}$ then the dimensionless parameter τ is given by $\tau \cong q^2/90$. The squared four-momentum transfer q^2 can be expressed through the energies E and E′ of the incident and scattered electron and the scattering angle Θ in the laboratory system in the following way

$$q^2 = 4 E E' \sin^2 \frac{\Theta}{2} \quad .$$

The cross-section

$$\left(\frac{d\sigma}{d\Omega}\right)_{NS} = \frac{\alpha^2}{q^2} \left(\frac{E'}{E}\right)^2 \frac{1}{tg^2 \frac{\Theta}{2}} \quad ,$$

occurring as a factor in the Rosenbluth equation, is the relativistic generalization of the Rutherford cross-section and gives the cross-section for the scattering of a relativistic electron in the pure Coulomb field of a hypothetical spinless particle of mass M.

Dr. Beckmann has discussed in his lectures the reasons why one prefers to use the electric and magnetic form factors $G_E(q^2)$ and $G_M(q^2)$ instead of the Dirac and Pauli form factors $F_1(q^2)$ and $F_2(q^2)$. There were essentially three reasons for this preference:

1. One advantage of using G_E and G_M instead of F_1 and F_2 is algebraic convenience. This is immediately apparent since G_E and G_M appear separately in the Rosenbluth equation, whereas if F_1 and F_2 are used the cross term $F_1 \cdot F_2$ appears. Thus, using G_E and G_M is of greater algebraic convenience when extracting form factors and errors out of the experimental data.

2. As was shown in Dr. Beckmann's lectures, the G_E^2 term corresponds to the exchange of a virtual photon with longitudinal polarization, whereas the G_M^2 term corresponds to the exchange of a virtual photon with transverse polarization. Longitudinal polarization implies zero angular momentum transferred along the direction of the virtual photon exchanged in the scattering process. Transverse polarization implies one unit of angular momentum transferred along that direction. When the exchanged photon carries one unit of angular momentum along $\vec{q}$ the nucleon spin must be flipped in the course of the scattering process with respect to $\vec{q}$. Thus, the G_M^2 term is the spin-flip term in the Breit or brick-wall system.

3. According to Sachs, the form factors G_E and G_M may have a more fundamental significance than F_1 and F_2 when it comes to a physical interpretation of these form factors in terms of spatial distributions of charge and magnetization inside the nucleon. However, the physical interpretation of the form factors in terms of spatial distributions of charge and current "inside" the nucleon is by no means obvious and all attempts in this direction are more or less esoteric. In any case, the Sachs argument is highly controversial. As is known from atomic physics, form factors are introduced into non-relativistic problems as Fourier-transforms of a charge density. For example, scattering of low-energy electrons by atoms can be analysed in terms of a form factor which can be Fourier-transformed back to give the charge distribution in the atoms. One would like to follow the same procedure for electron-nucleon scattering, i.e. determine the Fourier-transforms of the measured form factors $G_E(q^2)$ and $G_M(q^2)$ in three-dimensional momentum space to find spatial distributions of charge and magnetization inside the nucleon. However, difficulties are caused by the recoiling nucleon. It is no problem to define spatial density distributions in three-dimensional space by choosing a co-ordinate system in which the fourth component $q_0 = i\Delta E$ of the four-momentum transfer vanishes. One such system would be the centre-of-mass system of target nucleon and electron, another the Breit or brick-wall system. At low momentum transfers the proton can be considered to be at rest

during the collision. If this were true for all momentum transfers, then a real physical meaning could be attached to the Fourier-transforms. However, at large momentum transfers the recoiling proton becomes relativistic. Since its velocity is then comparable to the speed of the probing electron, the motion of the proton during the scattering process can no longer be neglected. Therefore, the relation of the three-dimensional Fourier-transforms to any real physical spatial structure of the proton is quite unclear, and the Fourier-transforms of $G_E(q^2)$ and $G_M(q^2)$ in three-dimensional space may have only pictorial usefulness. This must not worry us since all that is needed to describe the electron-nucleon electromagnetic interaction in the one-photon approximation are just the four nucleon form factors.

Since the Rosenbluth cross-section contains as the only adjustable parameters the two form factors $G_E(q^2)$ and $G_M(q^2)$, two elastic e-p cross-section measurements at a fixed q^2-value but different scattering angles are needed to determine both G_E and G_M. This requires that we programme the scattering angle and incident energy in such a way as to satisfy the relation

$$q^2 = 4 E E' \sin^2 \frac{\Theta}{2} \quad .$$

For precise results one cross-section measurement should be made at a large scattering angle and low incident energy where the G_M^2 term dominates the cross-section. For the second measurement a small scattering angle and a correspondingly high primary energy should be selected to obtain the largest possible influence of the G_E^2 term on the cross-section. At a given four-momentum transfer, cross-section measurements at more than two scattering angles are, in principle, not needed but can serve to improve the accuracy of the form factors derived from the data. Measurements at more than two scattering angles can also be useful to check at least to some extent the validity of the one-photon exchange approximation.

What is the procedure used to derive G_E and G_M from the experimental data? We notice that for a fixed q^2 the term in parentheses in the Rosenbluth equation is a linear function of $tg^2\ \Theta/2$. This suggests the "Rosenbluth plot" in which the experimental cross-section $d\sigma/d\Omega$ is divided by the cross-section $(d\sigma/d\Omega)_{NS}$ and plotted versus $tg^2\ \Theta/2$. If the Rosenbluth equation is valid, this plot should be a straight line with a slope of $2\tau G_M^2$ and a positive intercept at $tg^2\ \Theta/2 = -\frac{1}{2}(1+\tau)$ which is equal to $G_E^2/1+\tau$.

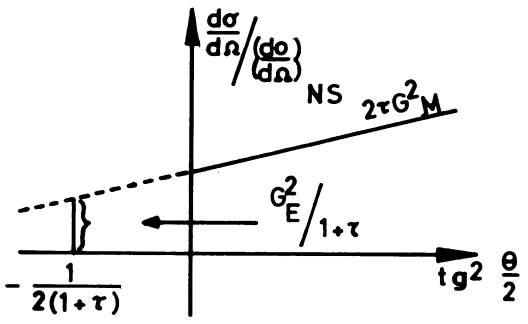

Thus, the slope gives $G_M^2(q^2)$ and the intercept $G_E^2(q^2)$. However, even if a straight line with a positive intercept at $tg^2\,\Theta/2 = -1/2(1+\tau)$ is found this does not necessarily prove the validity of the one-photon exchange approximation. Additional tests are necessary. Note furthermore that only the squares of the form factors can be determined in this way. However, the known values of the four nucleon form factors at zero four-momentum transfer plus the requirement that the form factors should be smooth functions of q^2 gives the sign of all nucleon form factors except for the electric form factor of the neutron G_E^n.

At $q^2 = 0$ the form factors G_E and G_M are normalized such that

$$G_E^p(0) = 1 \qquad G_M^p(0) = \frac{\mu_p}{\mu_K} \cong +2.79$$

$$G_E^n(0) = 0 \qquad G_M^n(0) = \frac{\mu_N}{\mu_K} \cong -1.91 \,.$$

Since the total charge of the neutron is zero, the sign of the electric neutron form factor cannot be obtained this way.

At sufficiently large scattering angles the second term in the Rosenbluth equation always dominates the cross-section. At a scattering angle of 180° the cross-section becomes

$$\frac{d\sigma}{d\Omega}(180°) = \frac{\alpha^2}{q^2}\left(\frac{E'}{E}\right)^2 \frac{1}{tg^2\,\frac{\Theta}{2}} \cdot 2\,\frac{q^2}{4M^2}\,tg^2\,\frac{\Theta}{2} \cdot G_M^2$$

$$= \frac{\alpha^2}{2}\,\lambda\!\!\!^{-2}_N \left(\frac{E'}{E}\right)^2 \cdot G_M^2 \simeq 1.2 \cdot 10^{-32}\left(\frac{E'}{E}\right)^2 G_M^2 \left[\frac{cm^2}{sr}\right] ,$$

where $\lambda\!\!\!^{-}_N$ is the nucleon Compton wavelength. For primary electron energies $E \gg M$ the ratio E'/E is approximately given by $M/2E$. Thus, G_M^2 can be determined directly from a 180° scattering experiment. According to my knowledge one such experiment has, in fact, been performed. However, in general, G_M^2 is obtained by the outlined method which requires measurements at <u>two</u> scattering angles for a fixed q^2-value.

When we discuss the available results on nucleon form factors we shall see that the magnetic form factor of the proton is known to a much higher accuracy than the electric form factor, especially at momentum transfers above 1 $(GeV/c)^2$. Why is this so? At large angles, i.e.

$$tg^2\,\frac{\Theta}{2} \gg \frac{(G_E/G_M)^2 + \tau}{2\tau(1+\tau)}$$

the elastic scattering cross-section is essentially determined by the second term in the Rosenbluth equation

$$\frac{d\sigma}{d\Omega}(\text{large angle}) \simeq \frac{\alpha^2}{2}\,\lambda\!\!\!^{-2}_N \left(\frac{E'}{E}\right)^2 \cdot G_M^2(q^2) \,.$$

The only energy dependence of the factor in front of G_M^2 is through the factor $(E'/E)^2$ and there is no angular dependence of the coefficient of $G_M(q^2)$ at all in this approximation. Thus, a systematic error in angle and/or energy would not affect the G_M value appreciably, but would lead to inaccurate G_E-values. This follows immediately from the G_E term in the Rosenbluth cross-section which is

$$\frac{d\sigma}{d\Omega}\,(G_E^2\text{-contribution}) = \frac{\alpha^2}{4}\,\lambda\!\!\!^{-2}\left(\frac{E'}{E}\right)^2 \frac{1}{tg^2\,\frac{\Theta}{2}}\;\frac{1}{\tau(1+\tau)}\cdot G_E^2 \quad .$$

The coefficient of G_E^2 is very sensitive to the measurement of angle and energy. This is one of the reasons why G_E is so poorly known compared with G_M. Secondly, it can be seen from the Rosenbluth equation that a good determination of G_E requires a measurement at a small angle and correspondingly high incident energy, since at small angles the cross-section is most sensitive to G_E. The ratio of the coefficients of G_E^2 and G_M^2 in the Rosenbluth equation as a function of angle for fixed q^2 values is given in Fig. 1. We see that the influence of the G_E^2 term on the cross-section increases with decreasing scattering angle. But, assuming that the incident energy is available, we see that even at small angles, i.e.

$$tg^2\,\frac{\Theta}{2} \ll \frac{(G_E/G_M)^2 + \tau}{2\tau(1+\tau)} \quad ,$$

the cross-section is not given by G_E^2 alone but by $G_E^2 + \tau G_M^2$. Since the relative contribution of the G_E^2 term cannot exceed the value $1/(1+\tau)$ we also see that the influence of the G_E^2 term decreases with increasing q^2. The influence which G_E^2 and G_M^2 may have on the cross-section can also be judged from Fig. 2 where the ratio of the coefficients of G_E^2 and G_M^2, as given by the Rosenbluth equation, is plotted versus scattering angle for various fixed incident electron energies[2]. Until recently, the required high energies for precise G_E measurements at momentum transfers above about 1 $(GeV/c)^2$ were not available. But with the 6 GeV electron beams now available at CEA and DESY one may hope that measurements at small electron scattering angles will yield more precise G_E values at momentum transfers above 1 $(GeV/c)^2$. Whether it really will be possible to derive more accurate G_E values from high energy small-angle measurements depends to a large extent on the value of the ratio G_E/G_M. Either $G_E/G_M \ll 1$. Then the contribution of the G_E^2 term to the cross-section will always be small. In that case one will hardly be able to measure G_E precisely at large momentum transfers. Or $G_E/G_M \gtrsim 1$. Then the contribution of the G_E^2 term to the cross-section is appreciable at sufficiently small angles even at high momentum transfers.

Measurements at a fixed four-momentum transfer at very small angles and correspondingly high incident energies are also desirable in view of the fact that the obtainable statistical accuracy of the cross-section measurements increases with decreasing scattering angle. This is due to the fact that the elastic scattering cross-section at a fixed four-momentum transfer increases considerably with decreasing scattering angle. By measuring the cross-section at very small scattering angles and correspondingly high energies one might therefore be able to detect even a relatively small G_E^2 term contribution to the cross-section.

Electron-proton scattering experiments are basically simple and straightforward when an intense beam of high-energy electrons is available. Such beams exist at the linacs at Stanford and Orsay and at the electron synchrotrons at Cornell, Harvard, Frascati and DESY.

In a typical arrangement, as shown in Fig. 3, the collimated and almost monochromatic electron beam first traverses a proton target. Its intensity is measured by a Faraday cup, a secondary emission monitor, or a total absorption ionization chamber. Typically, the energy spread in the beam is 1% or less. Targets of liquid or high pressure gaseous hydrogen as well as polyethylene have been used. Various types of magnetic spectrometers have been designed to analyse the momentum spectrum of electrons scattered at a given angle in a given solid angle $\Delta\Omega$. If one studies elastic scattering the spectrometer is set to select elastically scattered electrons. One can, of course, also select the recoil protons, but when using this method at high energies it is, in general, more difficult to discriminate between elastic and inelastic events by momentum analysis. The Stanford and Orsay groups use 180° deflecting double-focusing spectrometers of the Siegbahn type weighing up to 200 tons. At Cornell, Harvard, and DESY a different type of spectrometer is used, consisting simply of one quadrupole magnet (Fig. 4) that focuses a point source of electrons - the target - to a line image. At this image, a long narrow scintillation counter is placed which, together with a lead obstacle located at the centre of the quadrupole, defines the accepted momentum and the momentum resolution of the spectrometer. The electrons finally pass through a detector system which serves to identify and count the electrons. In order to discriminate effectively against pions in experiments in which primary electrons with energies of a few GeV are used, it is necessary to employ a detector system consisting of scintillation counters, a gas Čerenkov counter and, in some cases, a shower detector. Measurements of elastic e-p scattering become more difficult the larger the momentum transfer, since the cross-section for elastic e-p scattering decreases rapidly with increasing momentum transfer. Furthermore, background discrimination becomes more and more difficult with increasing energy. The rapid decrease of the cross-section for elastic e-p scattering with increasing scattering angle is shown[2] in Fig. 5. These cross-sections were computed under the assumption that G_E^p and G_M^p decrease as q^{-2} at four-momentum transfers above $q^2 = 100\ f^{-2}$. As an example, the cross-section at an incident electron energy of 6 GeV and a scattering angle of 150°, corresponding to a four-momentum transfer of about $270\ f^{-2}$, is expected to be approximately $5 \cdot 10^{-38}$ cm^2/sr. This value is about two orders of magnitude smaller than the smallest cross-section which has been measured thus far in electron scattering work at CEA, and is comparable to the order of magnitude of cross-sections for neutrino-induced reactions. With the available primary electron intensities and conventional magnetic spectrometers, such cross-sections will yield counting rates between 1 and 10 elastic events per day. On the other hand, the total number of pions emitted in the same solid angle can be roughly 10^5 times larger than the number of elastically scattered electrons. Momentum analysis of the scattered particles, detection of scattered electron and recoil proton in coincidence (Fig. 4), and sophisticated detector systems are used to reduce this background, but high-momentum transfer experiments remain difficult. The low counting rates can be overcome only by constructing high-current electron accelerators like the Stanford monster or possibly by building large solid-angle magnetic spectrometers utilizing spark chambers.

In order to extract a cross-section from the experimental momentum spectrum of scattered electrons, a number of corrections have to be applied, most important of which are the so-called radiative corrections. They arise from the emission of real photons during the scattering, and the emission and reabsorption of virtual photons. Owing to the infra-red character of these processes the contributions to the radiative corrections due to the emission

of soft photons are most important. In most experiments only the scattered electrons are detected at certain selected angles and momentum analysed. The emitted photons are not detected. Without radiative effects the spectrum of elastically scattered electrons would be represented by a δ-function. Strictly speaking, this statement applies only in the limiting case of vanishing energy spread and angular divergence of the primary beam, zero target thickness, and zero angular acceptance of the spectrometer. If one includes radiative effects the scattered electrons will be more or less degraded in energy by emission of real photons, and the spectrum of scattered electrons is no longer represented by a δ-function.

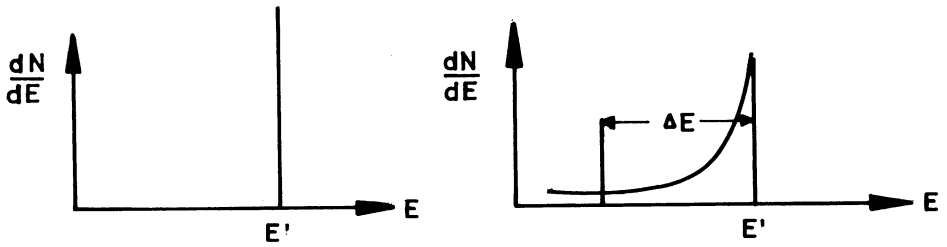

Instead, a momentum distribution with a long tail towards low energies is observed. The cross-section $d\sigma/d\Omega$ (ΔE) is obtained by integration over the double differential cross-section $d^2\sigma/d\Omega dE$,

$$\frac{d\sigma}{d\Omega}(\Delta E) = \int_{E'-\Delta E}^{E'} \frac{d^2\sigma}{d\Omega dE}\, dE \ .$$

We see from this that pure elastic scattering - elastic scattering without emission of real photons - is an idealization which does not occur in nature. The cross-section with $\Delta E = 0$ would be zero. In actual experiments the scattered electrons have a distribution in energy as shown

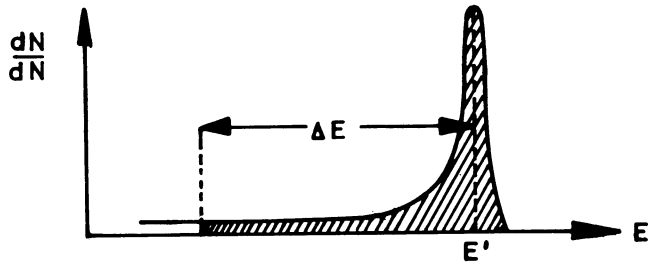

The typical shape of the low-energy part of the spectrum reflects the radiative losses during the scattering (radiative corrections) and emission of real bremsstrahlung. Since scattered electrons are only detected if the electrons have lost, by real photon emission, an amount of energy less than ΔE fixed by the experimental conditions (e.g. momentum resolution of the spectrometer or the energy cut-off) some "elastically" scattered electrons are lost. The only measurable cross-section is the cross-section for "elastic" scattering which includes the sum of the contributions from the radiative diagrams,

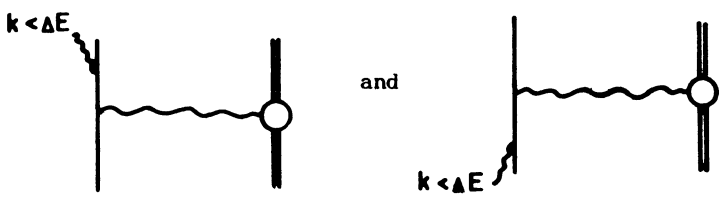

the electron vertex modification,

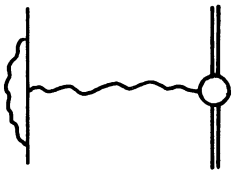

the vacuum polarization contribution,

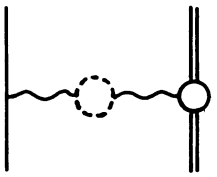

and higher order diagrams. Radiation from the proton current must also be included at momentum transfers $q^2 \gtrsim 1$ (GeV/c)^2. In order to compute the elastic e-p scattering cross-section $(d\sigma/d\Omega)_R$ from $d\sigma/d\Omega$ (ΔE) a correction must be applied, the magnitude of which will depend on the value of ΔE. The correction increases the cross-section which is represented by the shaded area under the curve on page 61. However, since all these diagrams are one-photon exchange diagrams the resulting cross-section is still completely determined by the two-proton form factors. Schwinger was the first to show that the measured cross-section $d\sigma/d\Omega$ (ΔE), represented by the shaded area under the curve, is related to the Rosenbluth cross-section for elastic e-p scattering by

$$\frac{d\sigma}{d\Omega}(\Delta E) = \left(\frac{d\sigma}{d\Omega}\right)_R (1 - \delta_{tot}) ,$$

where δ_{tot} is a complicated function of E, ΔE and Θ,

$$\delta_{tot} = \delta(E, \Delta E, \Theta) > 0 .$$

The experimental conditions are usually such that application of the radiative corrections amounts to an increase of the measured cross-section by about 15% to 25%, depending to some extent on primary energy, scattering angle, and accepted momentum band. This is demonstrated in Fig. 6 which is based on some recent numerical calculations by Kohaupt[3]. It shows the radiative correction δ_{tot} as function of scattering angle (or secondary energy) for 2, 4, and 6 GeV incident electron energy and various cut-off energies ΔE. In addition to the radiative corrections one has to correct for the radiation loss due to the emission of bremsstrahlung in the target which is proportional to the effective target thickness.

Thus far we have neglected the so-called two-photon exchange graphs. If two-photon exchange terms contribute significantly to the elastic e-p scattering cross-section it would certainly modify the interpretation of the data in terms of form factors

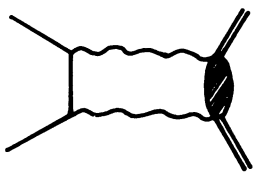

What evidence exists to justify the one-photon exchange approximation? This question should definitely be considered, especially at large momentum transfers, since the form factors become progressively smaller as q^2 increases. Furthermore, resonance enhancement effects may tend to equalize the one-photon and two-photon exchange terms.

If one includes a two-photon exchange term in the scattering amplitude, the elastic e-p scattering cross-section is given by

$$\frac{d\sigma}{d\Omega} \propto |\alpha A_1 + \alpha^2 A_2|^2 \ .$$

Since the one-photon exchange amplitude A_1 is real this yields

$$\frac{d\sigma}{d\Omega} \propto (\alpha A_1 + \alpha^2 \ \mathrm{Re}\ A_2)^2 + (\alpha^2 \ \mathrm{Im}\ A_2)^2$$

$$\simeq \alpha^2 A_1^2 + 2\ \alpha^3 A_1 \ \mathrm{Re}\ A_2 \ .$$

No theoretical predictions can be made about the two-photon exchange scattering amplitude A_2 without at least some knowledge of the structure of the nucleon. A typical two-photon exchange process is represented by a graph according to which one photon is exchanged which excites the nucleon to an isobaric state N^*,

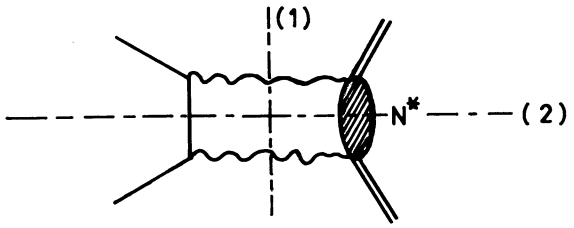

When exchanging the second photon, the nucleon returns to the ground state. If one cuts this graph vertically (cut 1), one has the product of Compton scattering of virtual photons by protons and Compton scattering of virtual photons by electrons. Cutting the diagram horizontally (cut 2) yields the product of two inelastic e-p scattering processes with excitation of an isobaric state N^*. Such models or cuts may enable us to estimate the contribution of such two-photon exchange graphs to the elastic e-p scattering cross-section. The result is that at electron energies up to at least 1 GeV the diagram corresponding to the excitation of the $\frac{3}{2}, \frac{3}{2}$ resonance is likely not to contribute more than about 1% to the total cross-section. This is due to the fact that the real part of A_2, as was discussed in Dr. Tripp's lectures, changes sign while going through the resonance. Therefore, upon integrating the virtual photon spectrum over the $\frac{3}{2}, \frac{3}{2}$ or any higher resonance the interference term $2\ \alpha^3 A_1 \ \mathrm{Re}\ A_2$ is largely cancelled and its net contribution is correspondingly small.

Heavy meson resonant states might also contribute to two-photon exchange terms

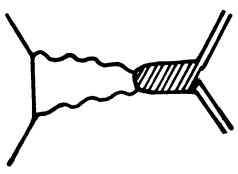

According to this two-photon exchange diagram the coupling between the two-photons and the nucleon is mediated by a meson resonance in the virtual meson cloud surrounding the bare nucleon. One could even think of a hypothetical direct coupling between electron and meson resonance. Unfortunately, it seems to be difficult to estimate at present in a reliable way the two-photon exchange scattering amplitude due to such a diagram. Therefore, it is important, especially at high momentum transfers, to consider the experimental evidence which exists to justify the one-photon exchange approximation.

The presence of two-photon exchange contributions might show up experimentally in three ways:

1. Deviations from the Rosenbluth plot which, if the one-photon exchange approximation is valid, should be a straight line with a positive intercept at $tg^2\,\Theta/2 = -1/2(1+\tau)$. As can be seen on Fig. 7 no evidence for a systematic departure from linearity or for a negative intercept at $tg^2\,\Theta/2 = -1/2(1+\tau)$ has been found in the investigated region of momentum transfers $q^2 \leq 45\ f^{-2}$. However, two qualifications should be made. First it should be mentioned that two-photon exchange terms can be invented for which the Rosenbluth plot remains a straight line with a positive intercept at $tg^2\,\Theta/2 = -1/2(1+\tau)$. Notice that this would completely change the interpretation of the plot in terms of electric and magnetic form factors. Secondly, as can be seen in Fig. 7, the linearity of the Rosenbluth plot has not been checked at laboratory angles below 90° for $25\ f^{-2} \leq q^2 \leq 35\ f^{-2}$. At $q^2 = 40\ f^{-2}$ and $45\ f^{-2}$ the minimum laboratory angle is 120°, and the Rosenbluth plot for $q^2 = 45\ f^{-2}$ ($\tau \simeq 1/2$) is just compatible with a zero or slightly positive intercept at $tg^2\,\Theta/2 = -1/3$. On the other hand, Gourdin and Martin[4] and Flamm and Kummer[5] have shown that, if the coupling through two-photon exchange is mediated by a hypothetical $J^{PC} = 1^{++}$ or 2^{++} intermediate state, a deviation from the linear Rosenbluth plot is to be expected but should only be measurable at small scattering angles. As Gourdin and Martin have discussed in their paper, for a $J^{PC} = 1^{++}$ intermediate state one arrives at a cross-section

$$\frac{d\sigma}{d\Omega} = \left(\frac{d\sigma}{d\Omega}\right)_{NS}\left[\frac{G_E^2 + \tau G_M^2}{1+\tau} + \left\{2\tau G_M^2 + c(\tau)\left(1 + \frac{1}{1+\tau}\cot g^2\frac{\Theta}{2}\right)^{1/2}\right\} tg^2\frac{\Theta}{2}\right]$$

where the additional term in the cross-section formula results from the interference term $2\alpha^3 A_1\ \mathrm{Re}\ A_2$. At angles corresponding to $tg^2\,\Theta/2 \gtrsim 1$ the deviation from the straight line behaviour is likely to be too small to be noticeable, although the cross-section itself may differ appreciably from the Rosenbluth value. To observe such a deviation which may exist at sufficiently large momentum transfers, one has to measure the cross-section at small angles and correspondingly high incident electron energies. Sufficiently high-energy beams were not available until recently but are now available at CEA and DESY. It is therefore not surprising that thus far no non-linearities have been detected. To summarize, we can conclude that due to a lack of small-angle measurements we do not have a good check that the real part of the two-photon exchange scattering amplitude is zero for $q^2 \gtrsim 1\ (GeV/c)^2$.

2. A second method of checking the presence or absence of two-photon exchange terms in elastic scattering is to compare the elastic scattering of positrons and electrons on protons. Since the difference between the cross-sections is caused by the interference term between the real single photon amplitude and the real part of the two-photon exchange amplitude, this

experiment again is sensitive to the real part of the amplitude of the two-photon exchange term. Measurements on electron-proton and positron-proton scattering were made[6] at Stanford up to momentum transfers of 19.5 f^{-2}. It was found that the ratio $\sigma_- - \sigma_+/\sigma_- + \sigma_+$, which is directly proportional to $\alpha^3 A_1 \text{ Re } A_2$, is equal to zero within the limits of error, implying that Re $A_2 \simeq 0$ for $q^2 \leq 19.5\ f^{-2}$. It would be worth while to check the validity of the one-photon exchange approximation by this method at much higher four-momentum transfers. But with the presently available positron beam intensities ($5 \cdot 10^8$ positrons per second) experiments of this kind can hardly be extended beyond momentum transfers of about 60 f^{-2}.

3. A third way to test the validity of the one-photon exchange hypothesis is to measure the polarization of the recoil proton which should be zero in the absence of two-photon exchange contributions. This experiment is also sensitive directly to the amplitude of the two-photon exchange term. The polarization of the recoil proton is perpendicular to the scattering plane and is proportional to

$$P \propto \alpha^3 A_1 \text{ Im } A_2 \ .$$

It is thus the imaginary part of the two-photon exchange term which gives rise to a polarization of the recoil proton in electron-proton scattering from unpolarized initial particles, whereas the difference between electron-proton and positron-proton cross-section was proportional to the real part of the two-photon amplitude. The two checks are thus not equivalent but supplement each other. Experiments to detect a possible polarization of the recoil proton in e-p scattering were performed at Orsay at a four-momentum transfer of 16.5 f^{-2} by Bizot et al.[7] and at Frascati at a momentum transfer of 20 f^{-2} by di Giorgio et al.[8]. In both experiments the polarization of the recoil proton was studied by measuring the left-right asymmetry in the scattering of the recoil protons in the carbon plates of a spark chamber. The result of both experiments was zero polarization within the limits of error. This means Im $A_2 \simeq 0$ at these four-momentum transfers and is in agreement with recent theoretical predictions[9]. It will be difficult to extend these measurements to higher four-momentum transfers because the efficiency for the polarization analysis decreases with the proton energy. A momentum transfer of 20 f^{-2} already corresponds to a recoil proton energy of 416 MeV. Furthermore, the e-p cross-section drops rapidly with increasing momentum transfer. Hopefully, polarization measurements may be feasible with presently available beam intensities up to four-momentum transfers of about 40 f^{-2}.

The present situation can be summarized in the following way. Although form factors are derived from electron-nucleon scattering work up to momentum transfers of 6.81 $(\text{GeV}/c)^2$ ($\hat{=}$ 175 f^{-2}) we have thus far no experimental justification that the one-photon exchange approximation is valid above four-momentum transfers of 20 f^{-2} or 0.8 $(\text{GeV}/c)^2$.

Next we shall discuss how one can obtain information on the electromagnetic structure of the neutron. Since we do not have dense enough free neutron targets, information on the neutron form factors is obtained mainly from high-energy electron-deuteron scattering experiments. Here one must distinguish between elastic e-d scattering and incoherent scattering of electrons from the loosely bound nucleons in the deuteron. Sometimes this second method is simply referred to as inelastic or quasi-elastic e-d scattering.

For elastic e-d scattering, the differential cross-section in the laboratory system is given by a modified Rosenbluth equation,

$$\frac{d\sigma}{d\Omega} = \left(\frac{d\sigma}{d\Omega}\right)_{NS} \left[A'(q^2) + B'(q^2)\ tg^2\ \frac{\Theta}{2} \right] ,$$

which again shows the linear dependence on $tg^2\ \Theta/2$. In the case of e-d scattering, however, the coefficients A′ and B′ depend on the squares of the three deuteron form factors. These three deuteron form factors are the charge form factor $G_E(q^2)$, an electric quadrupole form factor $G_Q(q^2)$, and a magnetic dipole form factor $G_M(q^2)$. Just as in the case of the proton, the coefficients A′ and B′ can be obtained from the Rosenbluth plot. It turns out that B′ depends only on the square of the magnetic form factor

$$B' = \frac{4}{3}\,\eta(1+\eta)\ G_M^2(q^2), \quad \text{with } \eta = \frac{q^2}{4M_D^2}$$

$$A' = G_E^2(q^2) + \frac{8}{9}\,\eta^2 G_Q^2(q^2) + \frac{2}{3}\,\eta(1+\eta)\ G_M^2(q^2) .$$

Thus G_M^2 can be obtained directly from the slope. The coefficient A′ depends on all three deuteron form factors. Unfortunately it is not possible to separate the charge and quadrupole form factors experimentally, but at small momentum transfers ($q^2 \lesssim 2.5\ f^{-2}$) the term containing the quadrupole form factor $G_Q(q^2)$ can be neglected, in which case G_E^2 can be derived from the Rosenbluth plot. To illustrate the behaviour of the three deuteron form factors as a function of q^2 we show in Fig. 8 the form factors calculated by Glendenning and Kramer[10].

However, here we are not interested in the form factors of the deuteron but in the form factors of the neutron. To use elastic e-d scattering to study the electromagnetic structure of the neutron requires a thorough understanding of the connection between the nucleon form factors and those of the deuteron. In order to establish this connection, one must make a number of simplifying assumptions. The most important of these are the use of the non-relativistic wave function of the deuteron and the assumption that the interaction of the virtual photon with meson exchange currents between the nucleons can be neglected. If we accept these approximations the deuteron form factors can be expressed in a simple manner in terms of the nucleon form factors. For example, the electric deuteron form factor G_E^D can be interpreted as

$$G_E^D = (G_E^P + G_E^n) \cdot F_D(q^2) ,$$

where $F_D(q^2)$, in the non-relativistic approximation, is the Fourier transform of $|\Psi_D|^2$. Here Ψ_D is the deuteron ground state wave function and $|\Psi_D|^2$ would describe the charge distribution inside the deuteron if the nucleons had no charge structure but were point particles. Since upon squaring the nucleon isoscalar form factor $(G_E^P + G_E^n)$ one obtains a cross-term $G_E^P \cdot G_E^N$, in principle experiments on elastic e-d scattering even allow one to establish the sign of the electric form factor of the neutron.

The electromagnetic structure of the neutron can also be studied in experiments on inelastic electron-deuteron scattering,

$$e + d \longrightarrow e' + n + p \quad .$$

The method is based on the idea that because of the loose binding of the nucleons in the deuteron, the inelastic electron-deuteron cross-section can be written approximately as the sum of the elastic electron-proton and electron-neutron scattering cross-section. In other

words, the deuteron, because of its extended structure and weak binding, acts as a reasonably good source of "quasi-free" neutrons. The problem can be treated in the so-called "impulse approximation". In this method the nucleons are considered as free particles, with a distribution of momenta caused by their binding within the deuteron. The cross-sections for scattering from the two nucleons are averaged over the initial nucleon momenta to give the total differential cross-section. However, the actual analysis of these experiments is complicated by many problems related to the detailed structure of the deuteron and to the final-state interactions between the emergent nucleons. One can distinguish the process of quasi-elastic scattering from elastic e-d scattering because of the fact that in this type of inelastic scattering the recoiling nucleon takes away much more energy than does the recoiling deuteron in elastic e-d scattering. Although the electrons scattered by the loosely bound nucleons in the deuteron are spread out to some extent in energy because of the Fermi motion of the nucleons inside the deuteron, the separation between the elastic peak and the inelastic continuum is such that discrimination between elastic and inelastic events is possible by momentum analysis of the scattered electrons. Because of the extended structure of the deuteron, the cross-section for elastic e-d scattering is small compared to the cross-section for incoherent electron-nucleon scattering at momentum transfers $q^2 >> 1/a^2$, where a is the deuteron rms radius.

By far the simplest way to investigate this type of scattering is to use the method in which only the scattered electron is detected. Since in first approximation the measured cross-section is given by the sum of the elastic electron-proton and electron-neutron cross-section, the elastic cross-section of the neutron is obtained by a simple subtraction of the e-p elastic cross-section. The e-p cross-section must therefore be measured simultaneously using a free proton target.

A more reliable method of determining the neutron form factors from inelastic e-d scattering is to detect both scattered electron and recoil neutron in coincidence. One selects the events with the recoil neutron momenta in a narrow cone around $\vec{q}$, the three momentum transferred from the electron to the nucleons in the laboratory system,

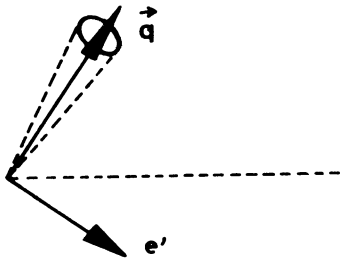

Since neutron detection is difficult it is experimentally often more convenient to replace the neutron counter by a high efficiency proton detector and register the number of anticoincidences. When using this method a scattered electron detected in anticoincidence is assumed to be an electron scattered by the neutron. The assumption is justified provided the proton counter covers a sufficiently large solid angle. At the same time, one also measures e-p coincidences from the deuteron target. The ratio of e-n to e-p scattering which is not so sensitive to experimental and theoretical uncertainties is then multiplied by the corresponding free proton cross-section to yield the neutron cross-section.

When discussing the experimental results we shall see that not only is the accuracy of the neutron form factors not as good as in the case of the proton but also there are obvious inconsistencies in the neutron data. This is especially the case for the electric form factor of the neutron. It is not too surprising in view of the following two facts:

1. Electron-deuteron scattering is generally dominated, especially at low momentum transfers, by the proton contribution. This is so since the magnetic moment of the neutron is smaller than the magnetic moment of the proton. Furthermore, $G_E^n(q^2) << 1$ at all momentum transfers. Thus, in most experiments one suffers from the fact that one must subtract two large and comparable cross-sections in order to find the small neutron cross-section. This implies large errors.

2. Although only loosely bound, the fact that the neutron instead of being free "sees" an extra proton introduces considerable theoretical uncertainties coming from meson exchange effects, the final state interactions between neutron and proton, and from the deuteron wave function which is not known precisely. Since the corresponding corrections cannot all be evaluated in a truly reliable way this introduces considerable uncertainties in the neutron form factors.

It thus appears that the present theoretical and experimental status of e-d scattering work is not sufficient to give truly reliable values of the neutron form factors.

We shall now discuss what is known experimentally about the behaviour of the nucleon form factors in the region of space-like momentum transfers.

A. Proton

Figure 9 shows a plot of G_E^p and $G_M^p/(1+\kappa_p)$ versus the four-momentum transfer q^2. The most recent experimental results on proton form factors are not contained in Fig. 9 but are given in Fig. 10 which extends up to four-momentum transfers of 6.8 $(GeV/c)^2$ or 175 f^{-2}. One notices immediately that $G_E^p(q^2)$ is not accurately known above momentum transfers of 1 $(GeV/c)^2$.

What major conclusions can be drawn from these figures?

1. For space-like momentum transfers G_E^p and G_M^p are smoothly decreasing functions of q^2, implying that the proton has structure. It is interesting to notice that $G_E^p(q^2)$ and $G_M^p(q^2/(1+\kappa_p)$ follow the same curve to within the experimental error at least up to four-momentum transfers of 1 $(GeV/c)^2$. At higher momentum transfers, $G_E^p(q^2)$ is not known well enough to prove or disprove this relationship. It is not known whether this empirical relation has any deeper meaning. At present we have no theoretical justification for this experimental result. We only know that the relation $G_E^p = G_M^p/(1+\kappa_p)$ can certainly not be valid at all four-momentum transfers since G_E^p and G_M^p must be equal to each other at a four-momentum transfer of $q^2 = -4M^2 (\tau = -1)$.

2. It is well known that the initial slope of the form factor curve versus q^2 is related to the rms radius of the corresponding spatial distribution. This is the reason why electron-nucleon scattering experiments at small momentum transfers are so important. From the slope of the proton form factor curves at $q^2 = 0$, one arrives at the conclusion that charge radius and magnetic radius of the proton are equal to within 2%. Both radii are 0.85 f and are thus considerably smaller than the pion-Compton wavelength $\lambda\!\!\!^{-}_{\pi} \simeq 1.4$ f.

3. The asymptotic behaviour of the nucleon form factors gives information about the possible existence of a "hard core" inside the nucleon. Furthermore, experiments on the form factor behaviour at large q^2 values can serve to check some of the current theoretical predictions on the asymptotic behaviour of form factors.

Using spatial concepts, one could imagine a concentration of a certain fraction of the nucleon charge or current density in the centre of the nucleon. Depending on the size of that volume, one would speak of a "hard core" (i.e. point-like concentration) or a "soft core". As is obvious from Figs. 9 and 10 both proton form factors decrease steadily towards asymptotic values which do not seem to be significantly different from zero. This behaviour implies that the proton has no hard core. This rejection of the hard core is considered to be the most important result of recent e-p scattering work. However, a "soft core" is not excluded by the data. It must be pointed out in this connection that at the largest momentum transfer that has so far been investigated, 6.8 $(GeV/c)^2$, it has only been possible to establish upper limits for the proton form factors. This is explained by the fact that up to now measurements at such a large momentum transfer have only been made at one angle, namely the smallest angle which could be selected with the existing apparatus at CEA. At the larger angles the cross-sections were too small to yield reasonable counting rates. Upper limits on the form factors were obtained by attributing the entire cross-section either to the G_M^2 term, thus putting G_E^2 equal to zero, or vice versa. In Fig. 10 the upper limit for $G_M/(1+\kappa_p)$ is given as an "inverted ground" at a four-momentum transfer of 6.81 $(GeV/c)^2$.

It would be very interesting to know in detail how the form factors decrease towards zero at large momentum transfers because this would make it possible to test a number of predictions based on different theoretical ideas. Dr. Beckmann has outlined in his lectures that according to dispersion theoretical ideas the asymptotic behaviour of the form factors may be expected to be given by the power law $1/q^2$. According to some other speculations it should be possible to relate e-p scattering at high four-momentum transfers to p-p scattering measurements which extend up to momentum transfers of 24.4 $(GeV/c)^2$. Yang and Wu suggested that the rapid decrease of the differential cross-section for p-p scattering with increasing momentum transfer is due to the fact that with increasing momentum transfer it is increasingly unlikely that the protons stay intact during the collision. Since in e-p scattering only one proton is involved and since furthermore the electron is not surrounded by an extended cloud of strongly interacting particles, Yang and Wu[11] speculate that the elastic e-p scattering cross-section should be proportional to the square root of the p-p scattering cross-section. This implies that the electromagnetic form factors of the nucleon could be proportional to the fourth root of the p-p scattering cross-section. According to Orear[12], the p-p scattering cross-section can be fitted quite well by

$$\left(\frac{d\sigma}{d\Omega}\right)_{pp} = A \cdot e^{-\frac{p \cdot \sin\Theta}{0.75}},$$

where the transverse momentum transfer $p_\perp = p \cdot \sin\Theta$ is expressed in units of inverse fermi. In order to establish the kinematical relationship between p-p and e-p scattering, Yang and Wu suggest that the transverse momentum transfer in p-p scattering should be replaced by $\sqrt{q^2}$ in e-p scattering. According to these speculations, the form factors should then decrease as $e^{-\sqrt{q^2}/3}$, where $\sqrt{q^2}$ is given in units of f^{-1}. As can be seen from Fig. 11 the experimental data can be fitted quite well by the exponential $e^{-\sqrt{q^2}/3}$ but the presently available experimental data are also compatible with a $1/q^2$ dependence in the asymptotic region.

B. Neutron

The neutron form factors are not as well known as the proton form factors mainly because of the difficulties in the theoretical interpretation of e-d scattering experiments. Elastic e-d scattering cross-sections have been measured up to momentum transfers of 0.3 $(GeV/c)^2$ or 8 f^{-2}. Inelastic e-d scattering data are available[13] up to q^2-values of 6.8 $(GeV/c)^2$ or 175 f^{-2}. However, the measurements at q^2-values $q^2 \geq 2.9$ $(GeV/c)^2$ or 75 f^{-2} yield only upper limits on the neutron form factors since at these large momentum transfers measurements have thus far only been made at one scattering angle. Some of the more recent neutron form factor values derived from inelastic e-d scattering work are given in Fig. 12. In this figure, G_M^n/κ_n and $(G_E^n)^2$ are plotted versus the four-momentum transfer q^2. The reason for plotting $(G_E^n)^2$ instead of G_E^n is that, because of the zero net charge of the neutron, the inelastic e-d scattering experiments do not allow us to determine the sign of G_E^n. Upper limits for the magnetic form factor of the neutron, including two standard deviation errors, are shown as inverted grounds in Fig. 12. The plot extends up to a q^2 of 4 $(GeV/c^2$, although upper limits on G_M^n are available up to momentum transfers of 6.8 $(GeV/c)^2$.

The available experimental information on the electromagnetic form factors of the neutron can be summarized as follows:

1. Both neutron form factors are smoothly varying functions of q^2. The relation $G_E = G_M/\kappa_n$ does not hold for the neutron in the range of four-momentum transfers where it was found to be valid in the case of the proton. For the neutron it is found that at least up to $q^2 \simeq 1$ $(GeV/c)^2$,

$$(G_E^n)^2 << \left(\frac{G_M}{\kappa_n}\right)^2 .$$

2. Just as in case of the proton, both form factors of the neutron seem to go towards asymptotic values at large momentum transfers which are not significantly different from zero. Therefore, a "hard neutron core" seems to be excluded. We do not know yet how rapidly the neutron form factors decrease with increasing momentum transfer. The magnetic form factor data which are thus far available in the asymptotic region can be fitted equally well by the power law $1/q^2$ or be the exponential $e^{-c\sqrt{q^2}}$.

3. The precise behaviour of the electric form factor of the neutron is unknown. According to the data obtained in inelastic e-d scattering experiments shown in Fig. 12, $(G_E^n)^2$ may be significantly different from zero and positive in the region of momentum transfers between 5 and 15 f^{-2}. Figure 13 gives some more neutron form factor data, especially in the region of small momentum transfers. The G_E^n values at $q^2 \leq 8$ f^{-2} were derived from elastic e-d scattering experiments and are compatible with the assumption $G_E^n(q^2) \equiv 0$. This is not only inconsistent with the electric form factor data shown in Fig. 12, but is also clearly inconsistent with the results of experiments on the scattering of thermal neutrons by electrons bound in atoms. According to these experiments, $(dG_E^n/dq^2)_{q^2=0} = +0.021$ f^2, which implies that $(G_E^n)^2 \cong 4.4 \cdot 10^{-4} \cdot q^4$ at small momentum transfers (q^4 is expressed in units of f^{-4}).

In order to demonstrate our lack of knowledge of G_E^n, a third plot of $(G_E^n)^2$ versus q^2 is shown in Fig. 14. These form factor data were derived by Hughes et al.[14]. He even obtained negative $(G_E^n)^2$ values for the neutron, a result which obviously makes no sense since the electromagnetic form factors must be real functions of q^2 in the

region of space-like momentum transfers. This clearly demonstrates that in spite of all the work which has been devoted in the last ten years towards the investigation of the neutron form factors, we do not yet know the detailed behaviour of G_E^n as function of q^2. All we know is that the electric form factor of the neutron is considerably smaller than unity at all momentum transfers investigated thus far. This is not inconsistent with SU_6 which predicts[15] that the ratio $G_E^n(q^2)/G_E^p(q^2)$ should be equal to zero. Since it is experimentally well established that $G_E^p(q^2) \neq 0$, SU_6 predicts $G_E^n(q^2) \equiv 0$. Thus far, the experiments have only shown that $G_E^n(q^2) \ll G_E^p(q^2)$ up to momentum transfers of 1 $(GeV/c)^2$. Also at higher momentum transfers, the SU_6 prediction is not excluded by the presently available experimental data.

SU_6 makes a second prediction, according to which the ratio of the magnetic form factors of the neutron and proton should be equal to the ratio of their magnetic moments which is minus $\frac{2}{3}$. As can be concluded from Fig. 14, the prediction is very well fulfilled at least up to four-momentum transfers of 30 f^{-2}.

With the exception of the electric form factor of the neutron, all electromagnetic form factors of the nucleon coincide, provided G_E^p and $G_M^{p,n}$ are normalized to 1 at $q^2 = 0$. This implies, as is summarized in Fig. 15, that the corresponding rms radii of proton and neutron agree within the experimental errors. They turn out to be 0.85 f.

As was discussed in Dr. Beckmann's lectures, one can try to understand the q^2 dependence of the electromagnetic form factors of the nucleon in terms of a vector-meson cloud surrounding the bare nucleon. The properties of the form factors in this model are thought to arise chiefly from the electromagnetic coupling of the photon to these heavy virtual vector mesons. This leads to the Clementel-Villi fit for the isoscalar and isovector form factors,

$$G(q^2) = G(0) - \sum_i \alpha_i + \sum_i \frac{\alpha_i}{1 + \frac{q^2}{m_i^2}} \quad ,$$

in which the constant term represents the contribution of a "hard core" and/or the contribution of very heavy hadrons, i.e. the "soft core". According to our present ideas, the virtual meson cloud is thought to be composed of the known vector mesons ρ, Φ and ω. These are considered to be the resonances which dominate the behaviour of the electromagnetic form factors in the space-like region but as long as one is not willing to treat the ρ mass as an adjustable parameter these three known vector mesons are not adequate to get a more or less satisfactory account of the nucleon form factors. If one treats the ρ mass as an adjustable parameter, a reasonably good fit of the experimental data up to at least $q^2 = 30\ f^{-2}$ is obtained for an effective ρ mass of about 550 MeV[14]. An alternative procedure is to introduce at least one more vector meson, called the ρ', with a fictitious mass of at least 950 MeV. But although quite a few new meson resonances have been reported in the recent literature none of these seems to have the proper quantum numbers to contribute to the isovector nucleon form factor ($J^{PC} = 1^{--}$, I = 1).

The most recent attempt to fit the form factor data with four-resonant states (ρ, φ, ω and the fictitious ρ') and no-core terms resulted in the expressions

$$G_{ES} = \frac{1.24}{1 + \frac{q^2}{15.8}} - \frac{0.74}{1 + \frac{q^2}{26.7}} \qquad G_{EV} = \frac{2.01}{1 + \frac{q^2}{14.5}} - \frac{1.51}{1 + \frac{q^2}{23.0}}$$

$$G_{MS} = \frac{1.12}{1 + \frac{q^2}{15.8}} - \frac{0.68}{1 + \frac{q^2}{26.7}} \qquad G_{MV} = \frac{6.23}{1 + \frac{q^2}{14.5}} - \frac{3.87}{1 + \frac{q^2}{23.0}}$$

where the mass values of the resonant states and q^2 are expressed in units of f^{-2} [13].

It may seem that there were a total number of eight adjustable parameters plus the mass value $m_{\rho'}$ of the fictitious vector meson ρ' with isospin 1. This, however, is not true. One has two constraints for the condition $G_E = G_M$ at $q^2 = -4M^2$, four constraints from the normalization condition at $q^2 = 0$ and one further constraint from the measured derivative of G_E^n with respect to q^2 at $q^2 = 0$. Thus, there remains only one free parameter plus the adjustable fictitious mass $m_{\rho'}$. The best fit is obtained for $m_{\rho'} = 945$ MeV $\hat{=}$ 23.0 f^{-2} but the fit is far from good. The fit can be improved by replacing the actual ρ mass of 760 MeV $\hat{=}$ 14.5 f^{-2} by a somewhat smaller effective ρ mass. If the fictitious isovector ρ' meson is omitted (one-pole approximation for the isovector form factor) the best fit is obtained for an effective ρ mass of about 550 MeV [14]. It is important to remember that one should not expect too good a fit since non-resonant pion states which are not included in the Clementel-Villi formula may contribute to the form factors. Furthermore, the Clementel-Villi form factor formula is obtained by replacing the spectral functions or weight functions of the vector resonant states by δ functions. This is a good approximation for the ω and φ meson but the approximation cannot be justified for the 100 MeV wide ρ state. These are some of the reasons why one should not attach too much importance to these fits. Remember that the more pole terms are included the more adjustable parameters are available. Every new vector meson brings into the fit a new pole term and its unknown coupling constants to the photon and the nucleon-antinucleon pair. The more resonant states are introduced, the better will be the fit, whether the theory is right or wrong.

REFERENCES

For more detailed information on the subject the reader is referred to:

S.D. Drell, Form factors of elementary particles, Rendiconti della scuola internazionale di fisica "E. Fermi" XXVI corso (1964).

R. Hofstadter and L.I. Schiff, Nuclear Structure, Stanford (1964).

L.N. Hand, D.G. Miller and R. Wilson, Revs. Modern Phys. 35, 335 (1963).

R.R. Wilson and J.S. Levinger, Ann.Rev.Nucl.Sci. 14, 135 (1964).

R. Hofstadter, Nuclear and Nucleon Structure, W.A. Benjamin, Inc., New York (1963).

T.A. Griffy and L.I. Schiff, Electromagnetic form factors, HEPL-363, ITP-155, Stanford, California (1965).

Furthermore, the reader is referred to the plenary sessions of the International Conference on Elementary Particles, Sienna (1963), to the plenary sessions of the International Conference on High-Energy Physics, Dubna (1964), and to the original papers in Phys.Rev. Letters.

1) R.B. Blumenthal et al., Bull.Am.Phys.Soc. 10, (series II), 445 (1965).
R.B. Blumenthal, Thesis, Harvard University, Cambridge (1965).

2) A. Boyarski and F. Bulos, SLAC-report TN/64-37.

3) R.D. Kohaupt, private communication.

4) M. Gourdin and A. Martin, CERN 4804/p/Th. 261, Rev.

5) D. Flamm and W. Kummer, Nuovo Cimento 28, 33 (1963).

6) A. Browman and J. Pine, Proc.Int.Conf. on Nucleon Structure, Stanford (1963), p. 85.
D. Yount and J. Pine, Phys.Rev. 128, 1842 (1962).

7) J.C. Bizot et al., Phys.Rev. Letters 11, 480 (1963).

8) G. di Giorgio et al., to be published, private communication by Dr. Ganssauge, DESY.

9) F. Guérin and C.A. Piketty, Nuovo Cimento 32, 971 (1964).

10) N.K. Glendenning and G. Kramer, Phys.Rev. 126, 2159 (1962).

11) C.N. Yang and T.T. Wu, Phys.Rev. (to be published).

12) J. Orear, Phys.Rev. Letters 12, 112 (1964).
A.D. Krisch, Phys.Rev. Letters 11, 217 (1963).
D.S. Narayan and K.V.L. Sarma, Phys. Letters 5, 365 (1963).

13) J.R. Dunning et al., Phys.Rev. Letters 13, 631 (1964).

14) E.B. Hughes et al., Phys.Rev. (to be published).

15) K.J. Barnes et al., Phys.Rev. Letters 14, 82 (1965).

16) M. Abolius et al., Phys.Rev. Letters 11, 381 (1963).
D.D. Carmony et al., Phys.Rev. Letters 12, 254 (1964).

Figure Captions

Fig. 1 Ratio A/B of electric and magnetic coefficients in Rosenbluth formula $d\sigma/d\Omega = AG_E^2 + BG_M^2$ versus electron scattering angle for fixed q^2 values. Dotted curves indicate accessible region for various incident electron energies.

Fig. 2 Ratio A/B of electric and magnetic coefficients in Rosenbluth formula $d\sigma/d\Omega = AG_E^2 + BG_M^2$ versus electron scattering angle for fixed incident electron energies. Four momentum transfers can be derived from right hand diagram[2].

Fig. 3 Typical experimental arrangement for the investigation of electron-nucleon scattering.

Fig. 4a and 4b The quadrupole spectrometers for the investigation of electron-nucleon scattering using an internal electron beam at DESY/Hamburg.

Fig. 5 Cross-sections for elastic e-p scattering. Above $q^2 = 100\ f^{-2}$ extrapolated cross-sections are given assuming that both proton form factors decrease as $1/q^2$ with increasing momentum transfer[2].

Fig. 6 Radiative corrections for elastic e-p scattering at small angles[3].

Fig. 7 Experimental "Rosenbluth plots".

Fig. 8 The calculated deuteron form factors of Glendenning and Kramer[10] versus the four-momentum transfer q^2.

Fig. 9 Proton form factors versus q^2 (N.F. Ramsey, Proc. of the Intern. Conf. on High Energy Physics, Dubna 1964).

Fig. 10 Proton form factors versus q^2 at large momentum transfers[13].

Fig. 11 Proton form factors G_E^p and G_M^p versus $\sqrt{q^2}$ [11].

Fig. 12 Neutron form factors at large four-momentum transfers obtained from inelastic e-d scattering[13].

Fig. 13 Neutron form factors at small four-momentum transfers.

Fig. 14 Neutron form factors versus q^2 [14].

Fig. 15 Experimental derivatives of the nucleon form factors at $q^2 = 0$ and corresponding electric and magnetic rms-radii.

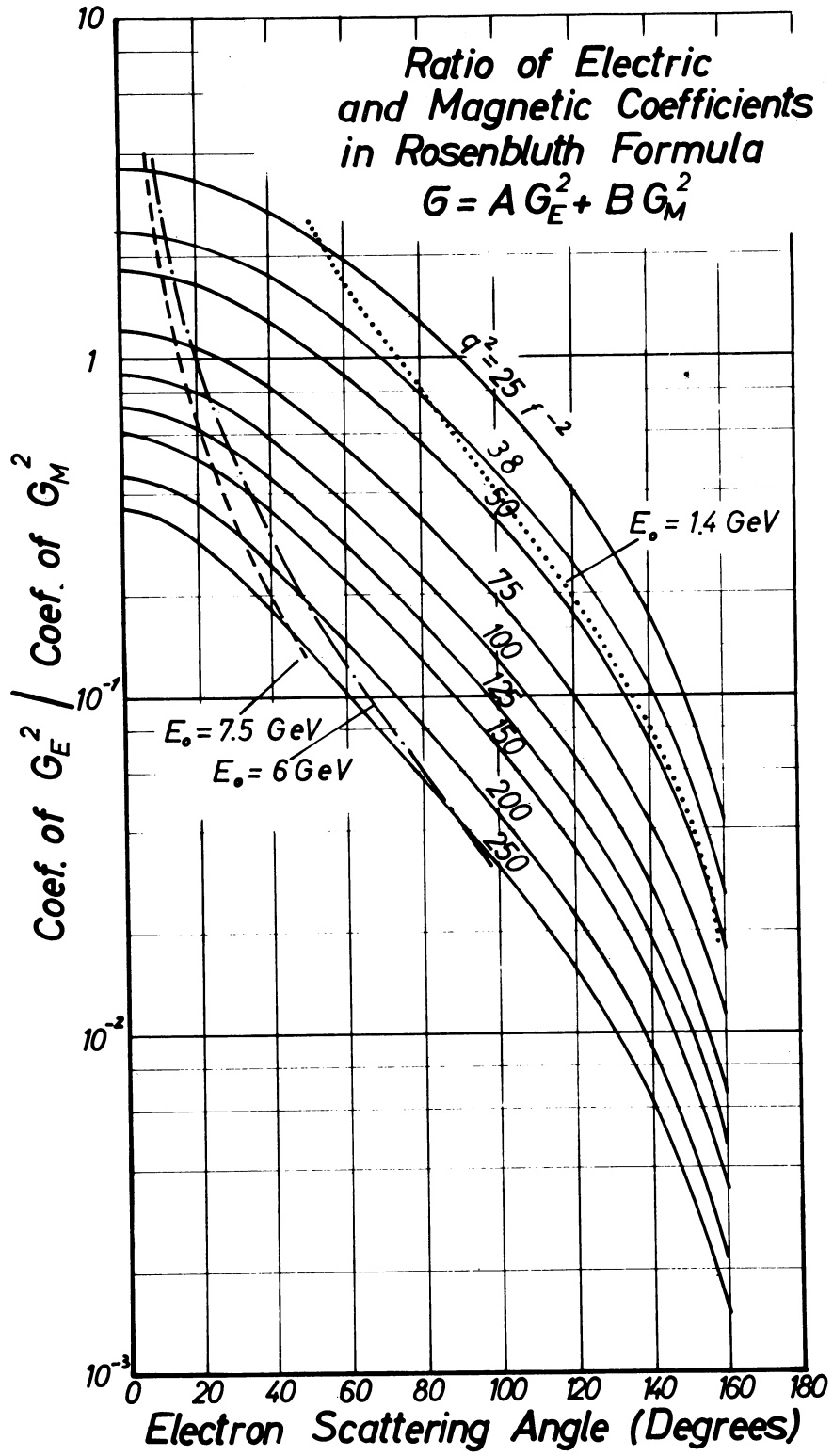
Ratio of Electric
and Magnetic Coefficients
in Rosenbluth Formula
$\sigma = A G_E^2 + B G_M^2$
$q^2 = 25\ f^{-2}$
38
50
75
100
125
150
200
250
$E_0 = 1.4$ GeV
$E_0 = 7.5$ GeV
$E_0 = 6$ GeV
Coef. of G_E^2 / Coef. of G_M^2
10
1
10^{-1}
10^{-2}
10^{-3}
0
20
40
60
80
100
120
140
160
180
Electron Scattering Angle (Degrees)

Fig. 1

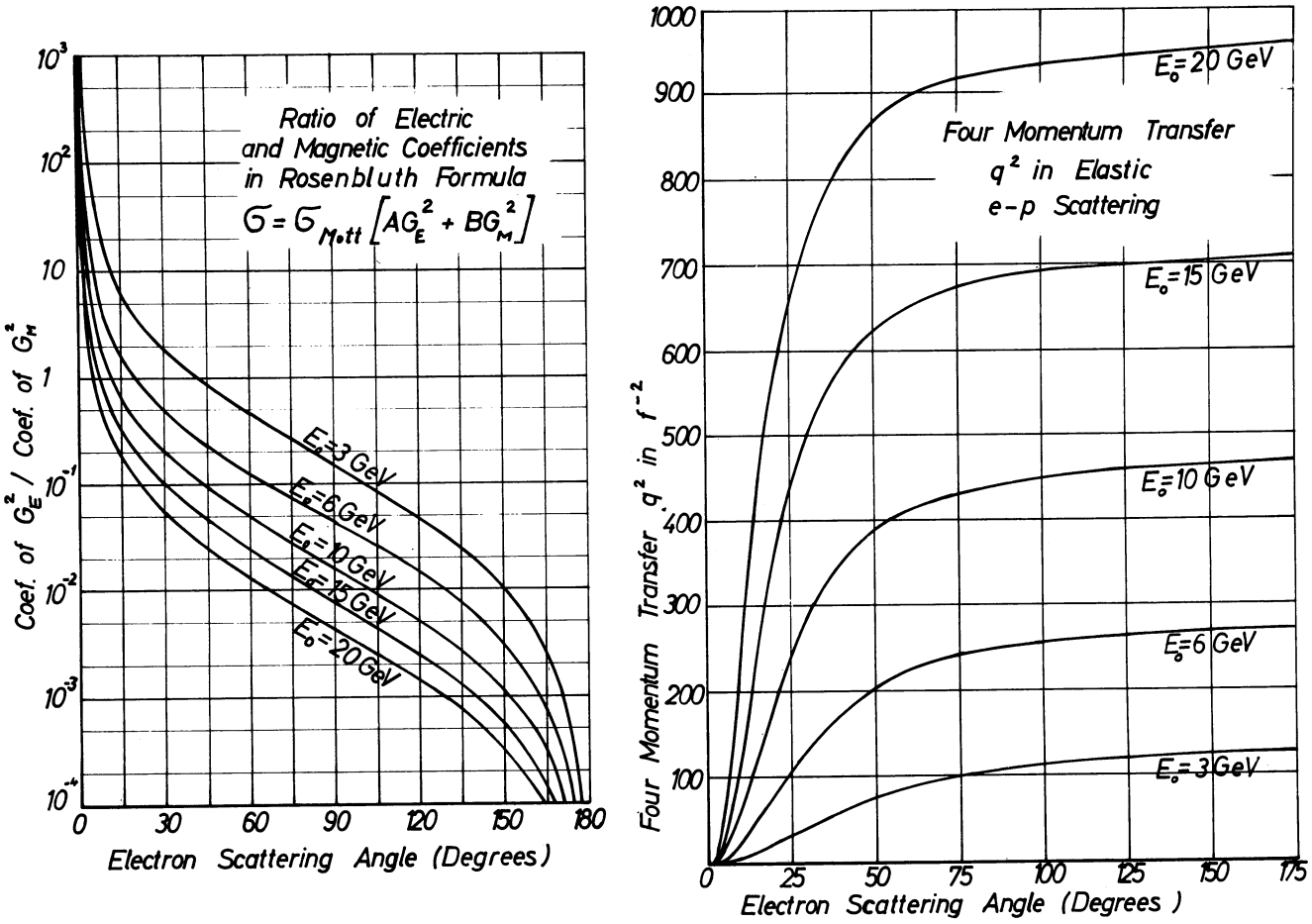
Ratio of Electric
and Magnetic Coefficients
in Rosenbluth Formula
$\sigma = \sigma_{Mott}\left[AG_E^2 + BG_M^2\right]$
E_0=3 GeV
E_0=6 GeV
E_0=10 GeV
E_0=15 GeV
E_0=20 GeV
Coef. of G_E^2 / Coef. of G_M^2
Electron Scattering Angle (Degrees)
Four Momentum Transfer
q^2 in Elastic
e-p Scattering
Four Momentum Transfer q^2 in f^{-2}
Electron Scattering Angle (Degrees)

Fig. 2

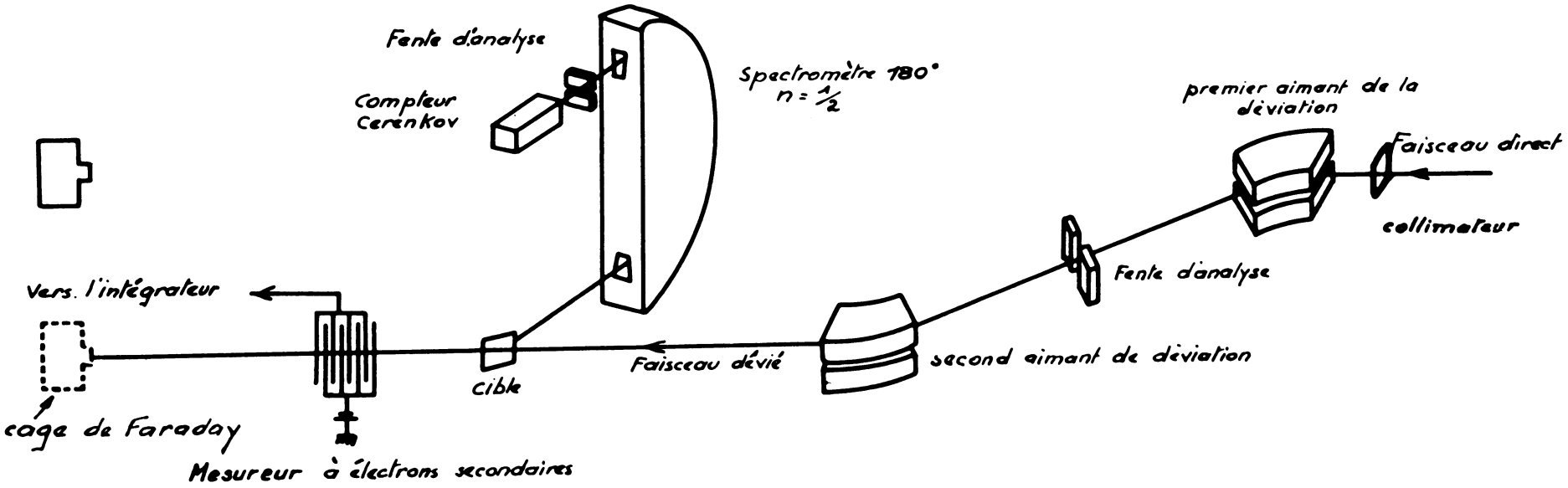
Fente d'analyse
Compteur Cerenkov
Spectromètre 180°
n = 1/2
premier aimant de la déviation
Faisceau direct
collimateur
Fente d'analyse
Vers. l'intégrateur
Faisceau dévié
second aimant de déviation
Cible
cage de Faraday
Mesureur à électrons secondaires

Fig. 3

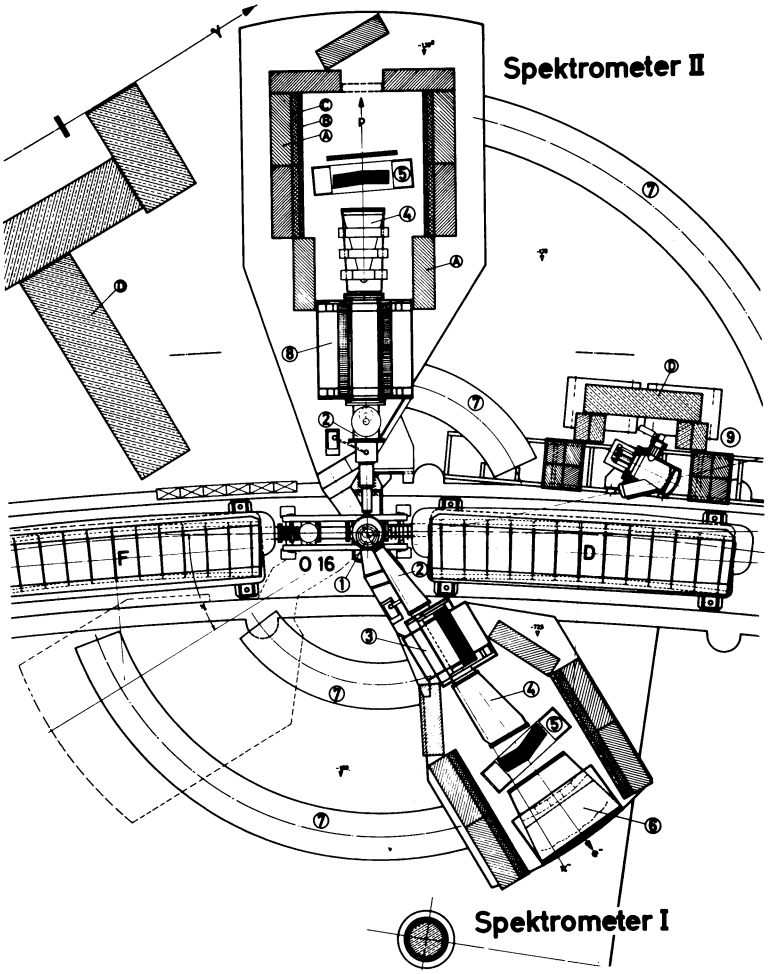
Spektrometer II
Spektrometer I
F
D
O 16

Fig. 4 a

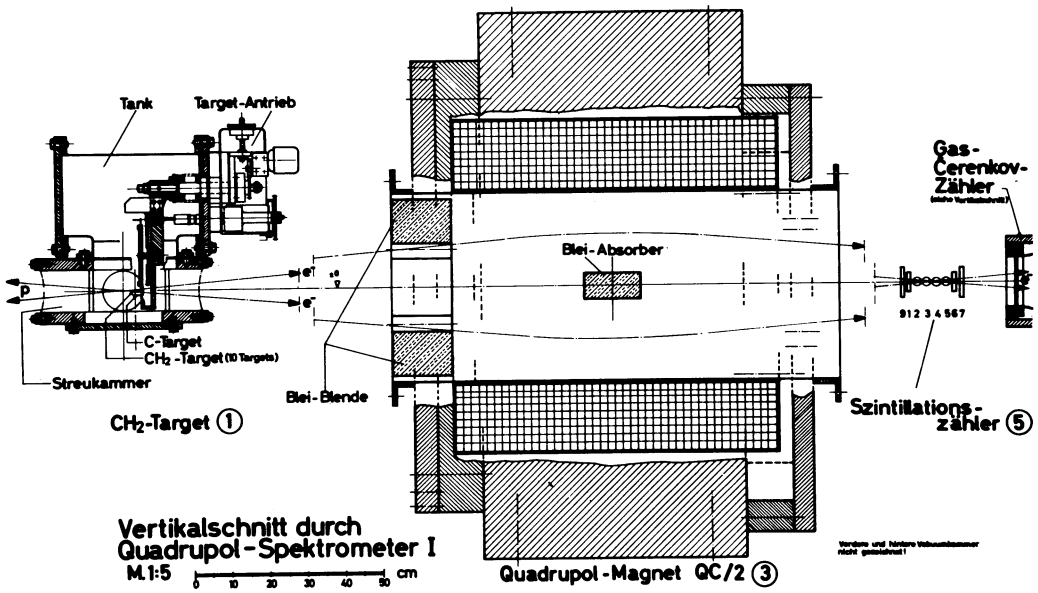
Tank
Target-Antrieb
C-Target
CH₂-Target (10 Targets)
Streukammer
CH₂-Target ①
Blei-Blende
Blei-Absorber
Gas-Cerenkov-Zähler
Szintillations-zähler ⑤
Vertikalschnitt durch
Quadrupol-Spektrometer I
M.1:5
0 10 20 30 40 50 cm
Quadrupol-Magnet QC/2 ③

Fig. 4 b

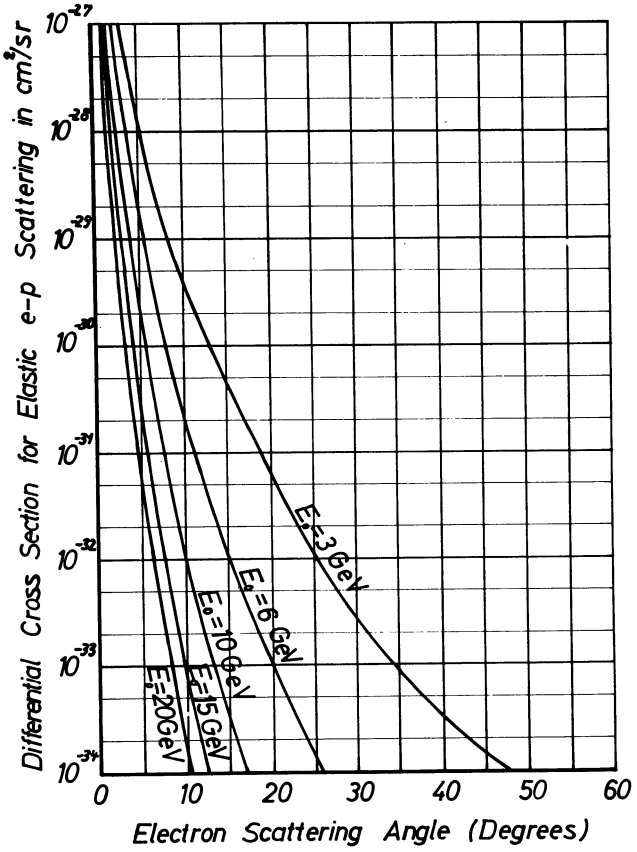
Differential Cross Section for Elastic e-p Scattering in cm²/sr
Electron Scattering Angle (Degrees)
E₀=3 GeV
E₀=6 GeV
E₀=10 GeV
E₀=15 GeV
E₀=20 GeV

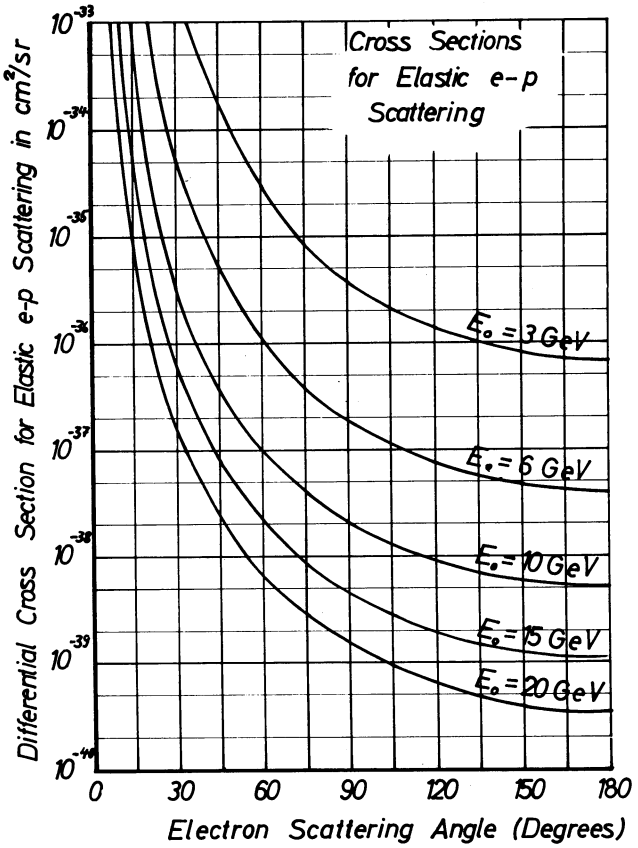
Cross Sections for Elastic e-p Scattering
Differential Cross Section for Elastic e-p Scattering in cm²/sr
Electron Scattering Angle (Degrees)
E₀ = 3 GeV
E₀ = 6 GeV
E₀ = 10 GeV
E₀ = 15 GeV
E₀ = 20 GeV

Fig. 5

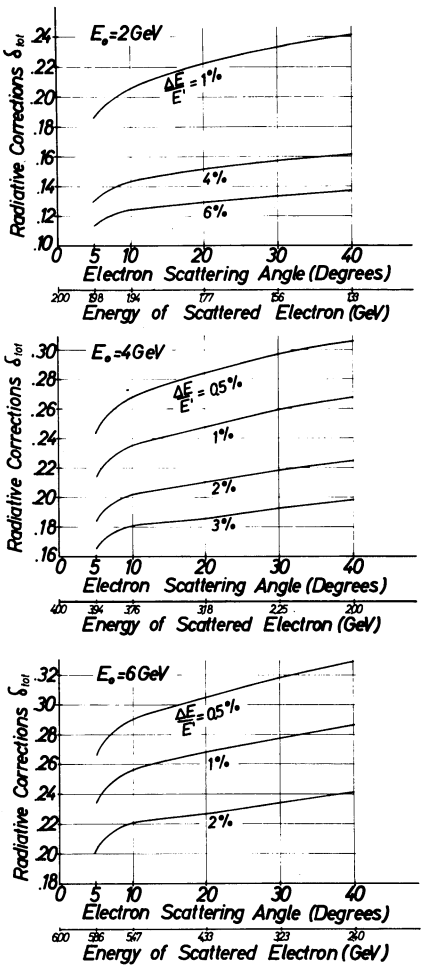
Radiative Corrections δ_{tot}
E_0=2GeV
$\frac{\Delta E}{E'}$ = 1%
4%
6%
Electron Scattering Angle (Degrees)
Energy of Scattered Electron (GeV)
E_0=4GeV
$\frac{\Delta E}{E'}$ = 0.5%
1%
2%
3%
E_0=6GeV

Fig. 6

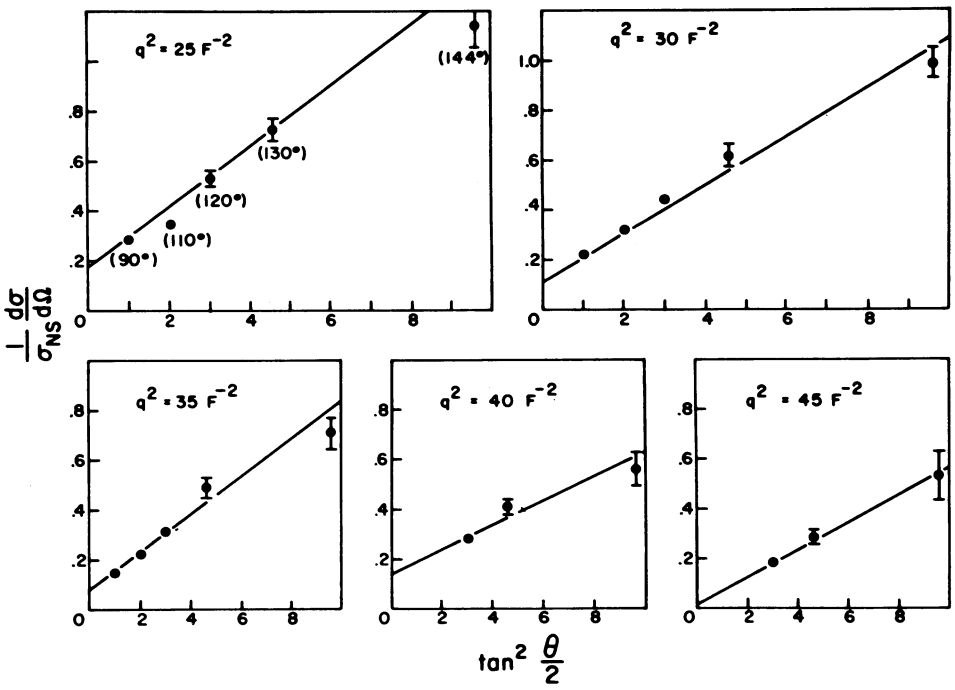
q^2 = 25 F^{-2}
q^2 = 30 F^{-2}
q^2 = 35 F^{-2}
q^2 = 40 F^{-2}
q^2 = 45 F^{-2}
(90°)
(110°)
(120°)
(130°)
(144°)
$\frac{1}{\sigma_{NS}} \frac{d\sigma}{d\Omega}$
$\tan^2 \frac{\theta}{2}$

Fig. 7

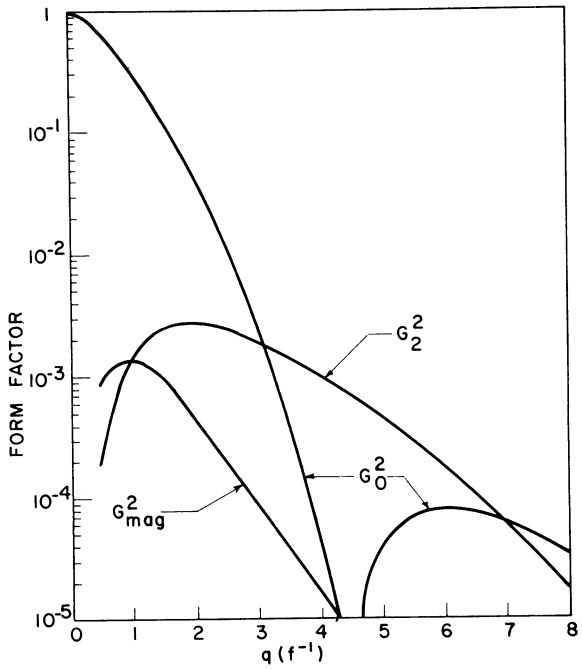

Fig. 8

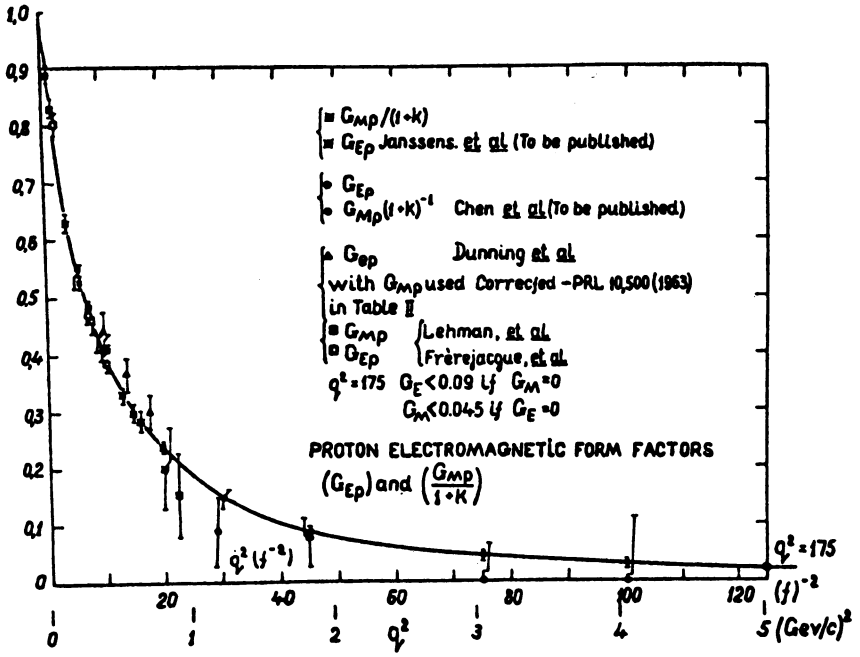

Electron-proton form factors.

Fig. 9

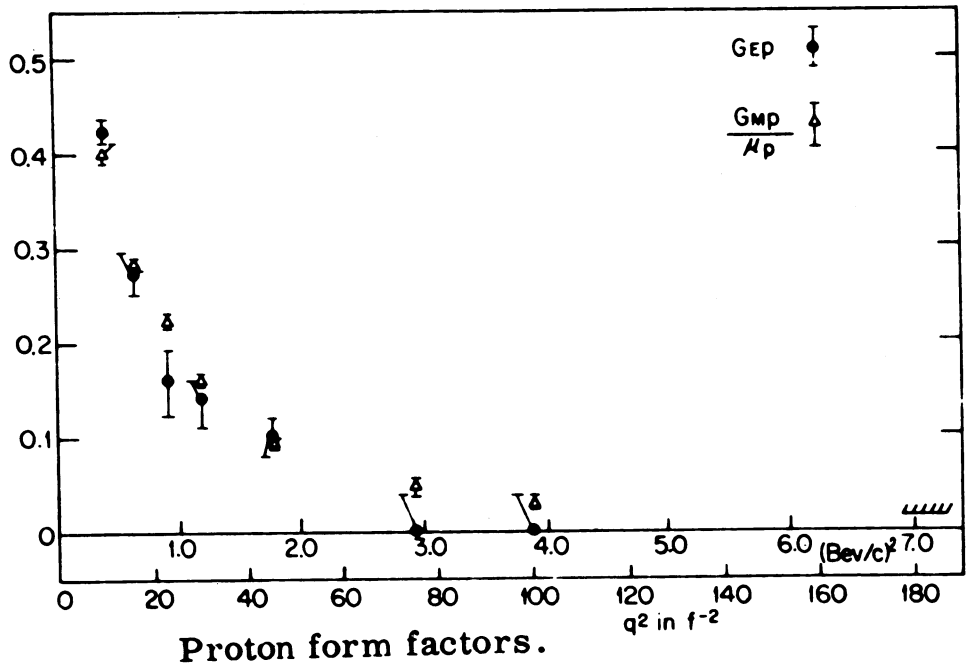

Proton form factors.

Fig. 10

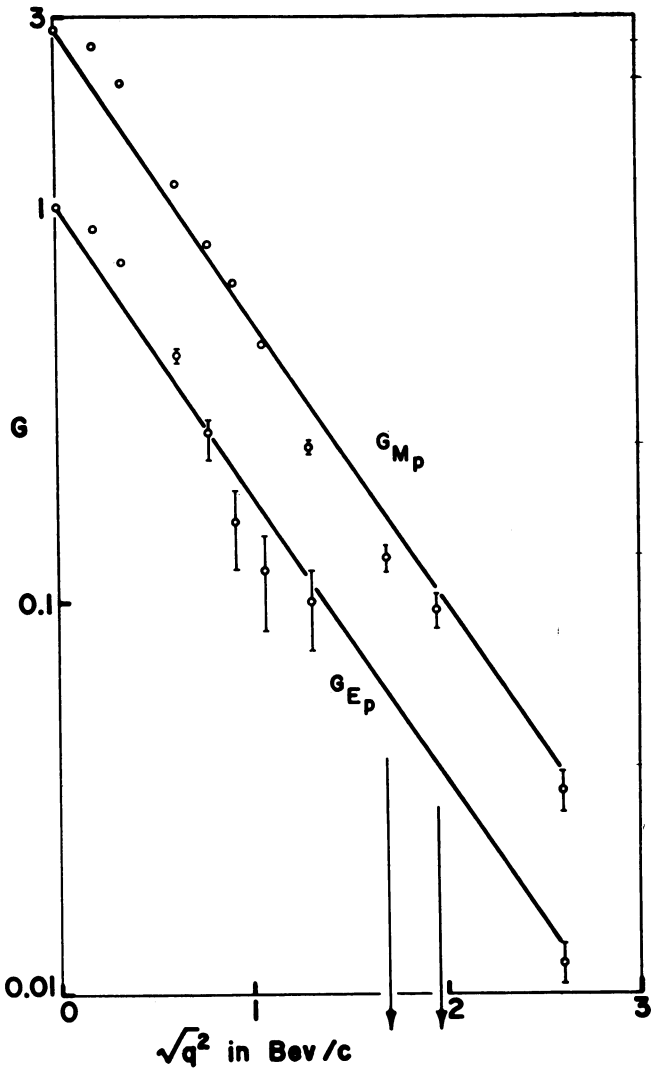

Fig. 11

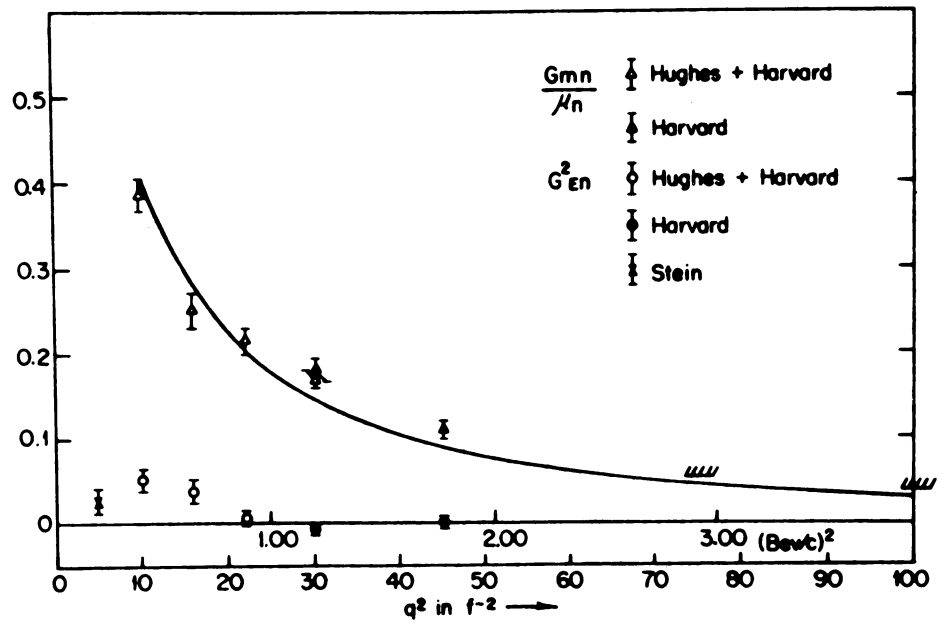
Gmn / μn
Hughes + Harvard
Harvard
G²En
Hughes + Harvard
Harvard
Stein
0.5
0.4
0.3
0.2
0.1
0
1.00
2.00
3.00 (Beut)²
0
10
20
30
40
50
60
70
80
90
100
q² in f⁻² ⟶

Fig. 12

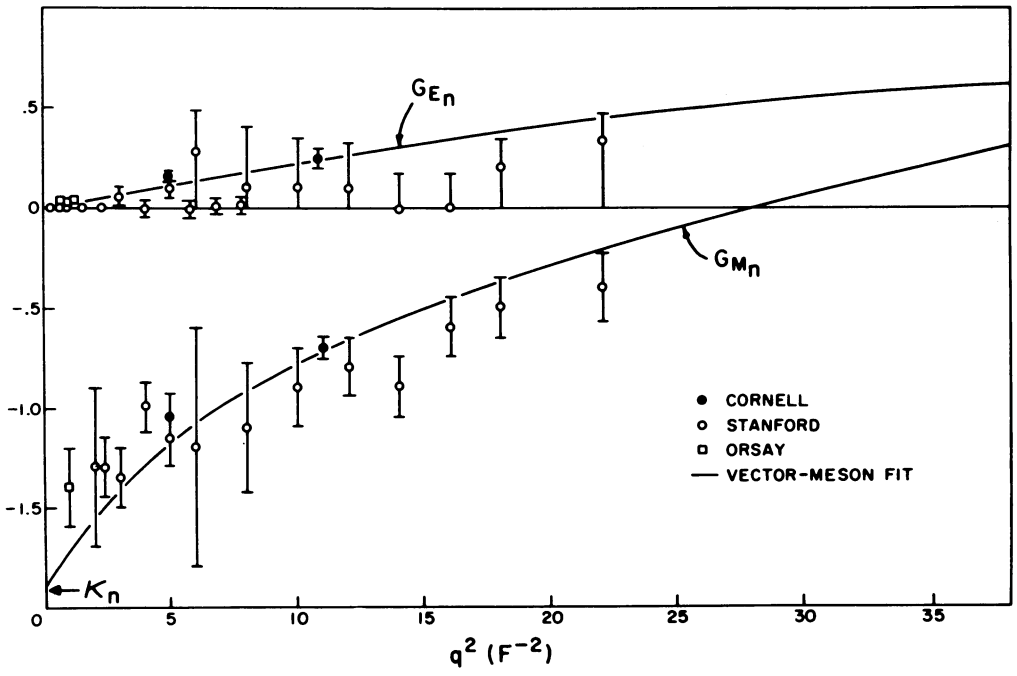
GEn
GMn
.5
0
-.5
-1.0
-1.5
Kn
CORNELL
STANFORD
ORSAY
VECTOR-MESON FIT
0
5
10
15
20
25
30
35
q² (F⁻²)

Fig. 13

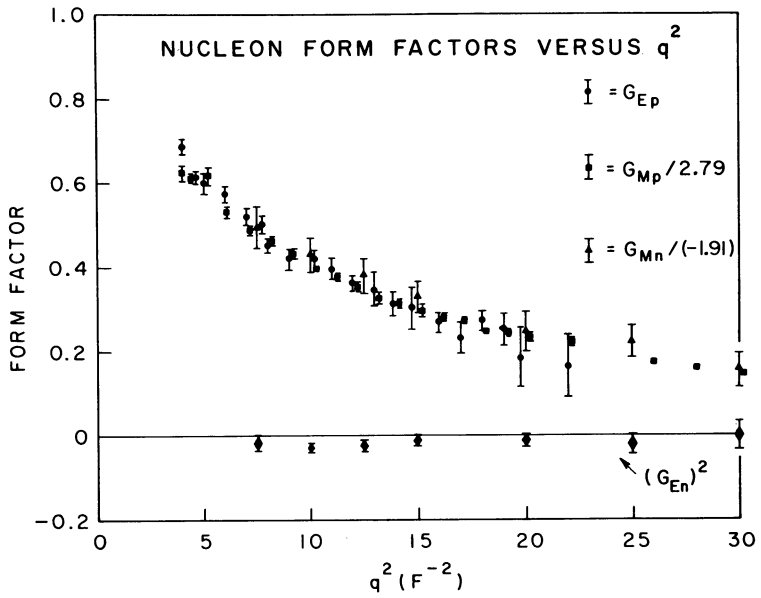

Fig. 14

EXPERIMENTAL DERIVATIVES OF THE FORM FACTORS AT ZERO MOMENTUM TRANSFER AND CORRESPONDING RMS-RADII

PROTON

$$\frac{dG_E^P}{dq^2}(0) = -(0{,}118 \pm 0{,}004)\, F^2 \qquad a_E^P = (0{,}84 \pm 0{,}01_5)\, F$$

$$\frac{dG_M^P}{dq^2}(0) = -(0{,}33 \pm 0{,}02)\, F^2 \qquad a_M^P = (0{,}85 \pm 0{,}02)\, F$$

NEUTRON

$$\frac{dG_E^n}{dq^2}(0) = +(0{,}021 \pm 0{,}001)\, F^2 \qquad a_E^n = (0{,}355 \pm 0{,}001)\, F$$

$$\frac{dG_M^n}{dq^2}(0) = +(0{,}26 \pm 0{,}09)\, F^2 \qquad a_M^n = (0{,}90 \pm 0{,}16)\, F$$

Fig. 15